



Development of recyclable, lightweight polypropylene-based single polymer composites with amorphous poly-alpha-olefin matrices

László József Varga, Tamás Bárány*

Department of Polymer Engineering, Faculty of Mechanical Engineering, Budapest University of Technology and Economics, Műgyetem rkp. 3., H-1111, Budapest, Hungary

ARTICLE INFO

Keywords:

A: Polymer-matrix composites (PMCs)
 A: Textile components
 B: Delamination
 B: Mechanical properties
 E: Isotactic pressing

ABSTRACT

In the present study, we produced and investigated polypropylene-based single-polymer composites (SPCs) using four amorphous poly-alpha-olefin (APAO) grades as matrices and two plain-woven polypropylene fabrics as reinforcement. Our goal was to investigate the applicability of APAOs as matrix materials of SPCs and to widen the processing temperature window of SPCs utilizing the low melting temperature of APAOs. We produced the composites with a double-belt press at 120 °C, 140 °C, and 160 °C, and investigated them by density measurement, and static tensile and dynamic falling weight impact (IFWI) tests at room temperature, -40 °C, and 80 °C. The composites showed adequate tensile and excellent dynamic mechanical properties. The tensile test results indicated that the optimal consolidation temperature is between 120 °C and 140 °C, depending on the matrix applied. Increasing the test temperature resulted in reduced tensile strength. Increasing processing temperature caused a drop in perforation energy because of the reduced extent of the delamination of the better-consolidated composites. Both static and dynamic mechanical properties can be improved with the use of a stronger fabric. Furthermore, the processing temperature window can be widened with APAOs as matrix materials, and these single-polymer composites possess many beneficial properties.

1. Introduction

Nowadays, environmental consciousness is becoming more and more important [1,2]. The development of new lightweight materials is essential to reduce the ecological footprint, especially in the automotive industry, where carbon-dioxide emissions can be reduced with lighter cars. Polymers are often used in the automotive industry, as they not only possess low density and excellent impact properties, but thermoplastic polymers can be easily recycled via remelting [3,4]. The problem is that polymers have modest mechanical properties compared to those of other structural materials [5]. The incorporation of ceramic (most commonly glass) fibers can improve the tensile properties of polymer parts, but only at the cost of reducing impact properties.

Single-polymer composites (SPCs) are recyclable, fully thermoplastic materials, in which the matrix and the reinforcement belong to the same polymer family. As the reinforcement is also a polymer in SPCs, these materials preserve the excellent impact properties of the matrix, accompanied by a significant improvement in tensile properties. Due to the drawing, the reinforcing fibers of SPCs possess higher strength and melting temperature than the matrix. This temperature difference

provides a small processing window for forming SPCs, even if the matrix and the fibers are from the same material [6]. These composites also have low density and good fiber/matrix adhesion [7]; furthermore, they can be recycled via remelting [8].

SPCs are often characterized by the quality of their consolidation. Well-consolidated SPCs have low void content, and thus better tensile mechanical properties [9]. The concept of single-polymer composites was first presented by Capiati and Porter in 1975 [10]. Since then, several methods for producing SPCs have been developed. The most commonly used production methods are hot compaction [11–15], consolidation of coextruded tapes [16–18], and film-stacking [19–21]. Lately, the scientific interest has shifted towards injection molding due to its versatility, and the results are promising [22–24].

The most substantial problem of SPCs is the narrow processing temperature window, as the reinforcing fibers suffer relaxation at high processing temperatures, which reduces their reinforcing potential. The processing window can be widened with matrix/reinforcement combinations that are not the same but belong to the same polymer family. Several material combinations were investigated with all the above-mentioned processing technologies, except hot compaction, as hot

* Corresponding author.

E-mail address: barany@pt.bme.hu (T. Bárány).

<https://doi.org/10.1016/j.compscitech.2020.108535>

Received 25 May 2020; Received in revised form 26 September 2020; Accepted 30 October 2020

Available online 3 November 2020

0266-3538/© 2020 The Author(s).

Published by Elsevier Ltd.

This is an open access article under the CC BY-NC-ND license

(<http://creativecommons.org/licenses/by-nc-nd/4.0/>).

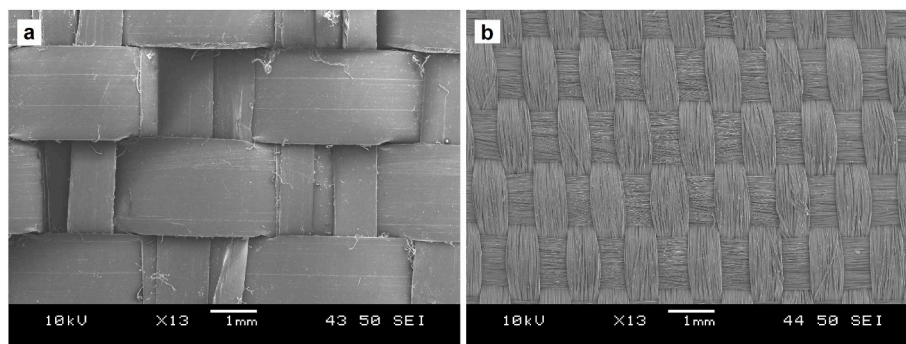


Fig. 1. Scanning electron microscopic images of Fabric 1 (a) and Fabric 2 (b).

compaction is based on the selective melting of the surface of the fibers. Consequently, the matrix and the reinforcement are always the same material in hot compacted SPCs [25].

The most commonly used material combination is homopolymer reinforcement with a copolymer matrix. In the case of polypropylene (PP), with the use of random polypropylene copolymer (rPP) as matrix and PP homopolymer as reinforcement, a processing window of approximately 15–20 °C can be achieved, depending on the exact copolymer type [19,26]. The combination of homopolymer reinforcement and copolymer matrix is also a viable solution to widen the processing window of poly (ethylene terephthalate) (PET) based SPCs [27, 28].

Some polymers show crystalline polymorphism, which also can be exploited to increase the melting temperature difference between the reinforcement and the matrix. In the case of polypropylene, the β crystalline form has a lower melting temperature than the α form. The melting temperature difference between the oriented reinforcement and the β -PP matrix is in the magnitude of 20 °C, and this difference can be even further increased with the use of an rPP matrix crystallized in the β form [29]. Several studies are available in the literature investigating the mechanical properties [30], the failure behavior [31,32], and the reprocessability [33] of these composites, reporting that they possess good tensile and excellent impact properties. The β -form can be produced by using selective β nucleating agents as additives [34].

We suggest a new matrix/reinforcement combination and exploit the low melting temperature of amorphous poly-alpha-olefins (APAOs) to widen the processing temperature window of polypropylene-based SPCs. APAOs were developed to substitute atactic polypropylene (aPP), which initially was a by-product of the production of isotactic polypropylene (iPP), but its availability decreased as stereospecific catalyst systems evolved, and less aPP was produced. Nowadays, APAOs

are produced on purpose with special catalyst systems, making it possible to specifically tailor their properties (e.g. viscosity, molecular weight). APAO molecules are mostly built by propylene repeating units ordered in an atactic manner, but APAOs are often copolymerized with other alpha-olefins (e.g. 1-butene, 1-hexene) [35]. APAOs are commercially available under the tradename of Vestoplast® (Evonik Industries, Germany) REXtac® (REXtac LLC, USA) or Eastoflex® (Eastman Chemical Company, USA). The main goal of this study is to investigate the applicability of four different APAO-grades as matrix materials for the production of single-polymer composites. The APAOs investigated have widely different viscosity and molecular weight.

2. Experimental

2.1. Materials and their processing

We used two kinds of woven fabric as reinforcement: Fabric 1 was composed of highly stretched split PP tapes (Fig. 1/a, Tiszatextil Ltd., Tiszajváros, Hungary), and Fabric 2 was composed of high-tenacity PP multifilament (Lanex a.s., Bolatice, Czech Republic). Fabric 2 was prepared by Csendes és Csendes Ltd. (Fig. 1/b, Szigetbecse, Hungary) upon our request. The main properties of the fabrics are listed in Table 1. We conduct all the tests with Fabric 1; Fabric 2 was only used in some cases for comparative purposes.

We used four different propene-rich amorphous poly-alpha-olefin-based melt adhesives as matrix materials: Vestoplast® 708, Vestoplast® 750, Vestoplast® 792, and Vestoplast® 888 (kindly provided by Evonik Resource Efficiency GmbH, Marl, Germany). These matrix materials are referred to as VP708, VP750, VP792, and VP888, respectively. These melt adhesives have widely different properties (Table 2).

Table 1

The properties of the reinforcing fabrics.

Fabric	Woven geometry	Areal density (g/m ²)	Warp/weft weight ratio (wt%)	T _m ^a (°C)	Tensile strength of single fiber/tape ^b (MPa)
Fabric 1	plain-woven	200	54/46	168.6	421 ± 27
Fabric 2	plain-woven	178	53/47	171.6	558 ± 26

^a Determined by DSC.

^b Measured on a single fiber/tape.

Table 2

Properties of the matrices.

Matrix	Melt viscosity (at 190 °C) (Pa s)	M _w (g/mol)	Density (g/cm ³)	Tensile strength (MPa)	Strain at break (%)	Glass transition temperature, T _g (°C) ^a	Melting temperature, T _m (°C) ^a
VP708	8 ± 2	75,000	0.87	1.0	330	-33	85.3
VP750	50 ± 4	92,000	0.87	5.0	1000	-29	79.8
VP792	120 ± 30	118,000	0.87	5.8	1200	-27	74.3
VP888	120 ± 40	104,000	0.87	2.5	850	-36	105.4/160.8

^a Based on DSC results.

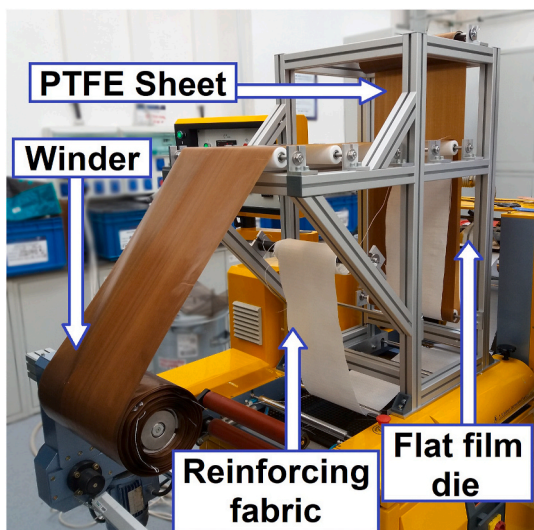


Fig. 2. The custom-built fabric-conveying apparatus.

Table 3

Perforation energy and shear modulus values of the matrices at different testing temperatures.

Matrix	Perforation energy (J/mm)		
	−40 °C	room temp.	80 °C
VP708	0.17 ± 0.09	4.65 ± 0.18	0.58 ± 0.07
VP750	0.20 ± 0.01	6.54 ± 0.33	0.51 ± 0.06
VP792	0.21 ± 0.02	7.00 ± 0.12	0.83 ± 0.05
VP888	12.30 ± 0.81	6.06 ± 0.15	1.27 ± 0.29

2.2. Preparation of composites

2.2.1. Fabric coating

We produced the composites similarly to the film-stacking method. The film-stacking method requires thin sheets of the matrix material, which will melt during the consolidation of the laminated pre-products, and become the matrix of the composites. These matrix sheets are usually produced by film extrusion. The low viscosity and extreme “stickiness” of amorphous poly-alpha-olefins make standard processing difficult, resulting in an unbalanced thickness of the matrix films [36]. To overcome this problem, we designed and built fabric conveying equipment (Fig. 2).

This device can be mounted on our film extrusion line (Fig. 2, Labtech LCR300, Labtech Engineering Co., Samutprakarn, Thailand). During production, the equipment guides the reinforcing fabric to the flat

Table 4

The fiber content, density, and peel strength of the composites.

Fabric	Matrix	Consolidation temperature (°C)	Fiber content (wt%)	Areal relaxation (%)	Density (g/cm ³)	Peel strength (N/mm)
Fabric 1	VP708	120	79.8 ± 1.5	5.3 ± 0.8	0.71 ± 0.01	0.31 ± 0.03
Fabric 1	VP708	140	79.9 ± 3.4	14.9 ± 1.9	0.71 ± 0.01	0.30 ± 0.04
Fabric 1	VP708	160	75.5 ± 2.0	38.6 ± 2.1	0.77 ± 0.01	0.24 ± 0.03
Fabric 1	VP750	120	78.3 ± 0.9	5.8 ± 0.5	0.70 ± 0.02	1.36 ± 0.14
Fabric 1	VP750	140	79.5 ± 2.8	15.3 ± 3.0	0.68 ± 0.01	1.25 ± 0.03
Fabric 1	VP750	160	71.0 ± 5.6	39.6 ± 7.1	0.78 ± 0.02	1.91 ± 0.23
Fabric 1	VP792	120	72.6 ± 5.3	4.3 ± 1.1	0.74 ± 0.03	1.50 ± 0.11
Fabric 1	VP792	140	75.1 ± 2.7	17.0 ± 2.5	0.77 ± 0.01	1.61 ± 0.09
Fabric 1	VP792	160	72.6 ± 1.7	37.6 ± 2.7	0.79 ± 0.01	2.44 ± 0.19
Fabric 1	VP888	120	90.3 ± 0.8	7.2 ± 0.1	0.75 ± 0.01	0.20 ± 0.11
Fabric 1	VP888	140	87.0 ± 2.7	14.1 ± 1.6	0.71 ± 0.01	0.40 ± 0.11
Fabric 1	VP888	160	86.6 ± 4.6	43.3 ± 5.8	0.81 ± 0.01	0.53 ± 0.03
Fabric 2	VP708	120	71.1 ± 1.4	4.9 ± 0.7	0.82 ± 0.01	n.m.
Fabric 2	VP792	120	73.4 ± 3.4	4.3 ± 0.5	0.74 ± 0.02	n.m.

film die of the extruder (Labtech LE 25–30C, Labtech Engineering Co., Samutprakarn, Thailand), where the matrix film is extruded directly onto the fabric. After extrusion, the coated fabric is guided towards the winder by polytetrafluoroethylene (PTFE) rollers while it cools down. To avoid the preform sheets sticking together, we placed a PTFE film between them during the winding process. The thickness of the matrix films—which determines the fiber content of the composites—is set by the rotating speed of the extruder screw, the distance between the die lips, and the pulling speed of the coated fabric. To determine the parameters to achieve the fiber content of 75 wt%, we conducted a preliminary test. In this test, the rotating speed of the extruder screw and the distance between the die lips were 70 1/min and 0.5 mm, respectively. The pulling speed of the coated fabric was altered in a wide range, with the step of 0.5 m/min, and the rotating speed of the winder was set accordingly. The temperature of the die was 120 °C for Vestoplast 708, 750, and 792 and 180 °C for Vestoplast 888 (stable production was only possible at this temperature). The first roll was tempered to 40 °C. We calculated the fiber content of the composites to be consolidated at each point and determined the required pulling speed to achieve the fiber content of 75 wt% by linear interpolation. Based on these results, the required pulling speeds are 7.4, 8.9, 5.5, and 9.0 m/min in the case of VP708, VP750, VP792, and VP888, respectively.

2.2.2. Composite preparation

Four layers of coated and one layer of uncoated fabric were placed on each other and consolidated in a double-belt press (DBP, Reliant Powerbond-HPC, Reliant, United Kingdom). Due to the “stickiness” of APAO, only one side of the reinforcing fabric was coated in our apparatus, so adding an uncoated fabric layer was necessary to form a symmetrical arrangement. During composite production, the pulling speed of the laminates was 1.5 m/min, and a pressure of 0.6 MPa was applied. The pressure of 0.6 MPa is the maximal adjustable pressure of the DBP. The composites were produced at 120 °C, 140 °C and 160 °C, and were given a name based on their matrix (VP708, VP750, VP792, and VP888). The fiber contents of the PP-SPCs differed from each other (Table 4), thus, to make the effects of the matrix on the properties of the composites comparable, tensile properties and perforation energy were normalized to 75 wt% fiber content, by multiplying the property of the composite sheet with the ratio of 75 wt% and the fiber content of the sheet. The composites were produced with Fabric 1, but in the case of VP708 and VP792, composites were also produced with Fabric 2 at 120 °C for comparative purposes.

2.3. Characterization methods

Differential Scanning Calorimetry was performed on the matrices and reinforcing fabrics with a Q2000 DSC device (TA Instruments, New Castle, United States) in a 50 mL/min nitrogen atmosphere, with a heating rate of 10 °C/min.

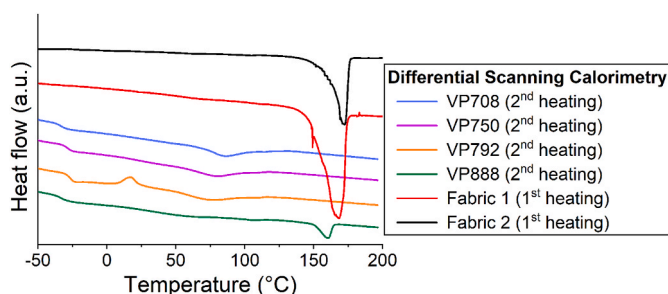


Fig. 3. DSC curves of the reinforcements and matrices, obtained from the 1st heating cycle for the fabrics, and 2nd heating cycle for the matrices.

The shear modulus of the matrices was measured with a DMA Q800 device (TA Instruments, New Castle, United States). We conducted the test according to the EN ISO 6721-2 standard on $10 \times 10 \times 2$ mm specimens with a shear sandwich clamp with a frequency of 1 Hz. The test was conducted from -60 to 100 °C, and the shear modulus was evaluated at room temperature, -40 °C and 80 °C.

The matrices and the composites were characterized by instrumented falling weight (IFWI) tests performed with a CEAST 9350 falling weight impact testing machine (Instron, Massachusetts, USA) with the following settings: the total mass of the dart: 28.41 kg, height: 1 m, impact energy: 278.65 J, dart diameter (semispherical): 20 mm, and diameter of the supporting ring: 40 mm. In the case of the matrix materials, we used $80 \text{ mm} \times 80 \text{ mm} \times 2 \text{ mm}$ injection molded (Arburg Allrounder 470 A, Arburg GmbH, Lossburg, Germany) specimens prepared with the injection pressure of 500 bar and the packing pressure of 300 bar. We used $110 \text{ mm} \times 110 \text{ mm}$ and $150 \text{ mm} \times 150 \text{ mm}$ square specimens in the case of the composites prepared with Fabric 1 and Fabric 2, respectively. The tests were performed at room temperature, -40 °C, and 80 °C.

The density of the composites was determined according to Archimedes' law in ethanol at 23 °C with $10 \text{ mm} \times 10 \text{ mm}$ specimens. To

determine the mass of the specimens, we used an Ohaus Explorer E01140 analytical scale (Ohaus Corporation, Nänikon, Switzerland), which has an accuracy of 0.1 mg.

The cross-section of the composites was investigated with a light microscope (VHX-5000, Keyence, Mechelen, Belgium). We embedded the composites in epoxy resin and polished the surface of the samples with a LaboPol-5 polisher device (Struers A/S, Denmark). The dimensions of the reinforcing tapes were measured with the software of the optical microscope.

The surface of the composites was investigated with a JEOL JSM6380LA scanning electron microscope (JEOL Ltd., Tokyo, Japan) with an accelerating voltage of 10 kV and a spot size of 40. The observed surfaces were sputter-coated with gold in an argon atmosphere.

We determined the peel strength of the composites with a Zwick Z020 (Zwick GmbH & Co., Ulm, Germany) universal testing machine by peeling off the side reinforcing layer of the composite sheets, using $25 \text{ mm} \times 300 \text{ mm}$ rectangular specimens. The machine was equipped with a 20 kN load cell, and we performed the test with a crosshead speed of 152 mm/min and a preload of 1 N. Although the standard suggests using a special peeling head which can be mounted on the crosshead of the tensile testing machine, due to the relatively low modulus of the composites, the specimens were fixed directly in the grips of the tensile testing machine; otherwise, the composites were "creased" in between the rolls of the standardized peel head. Consequently, the results of the peel test cannot be compared to the peel strengths of other fabric-reinforced composites. Nevertheless, the effect of the matrix material and the consolidation temperature on peel strength can still be investigated based on the peel test results. To initiate peeling, we inserted a thin PTFE film between the first and second coated fabric during the assembly of the layers. The peel strength was calculated with the average peeling force divided by the width of the specimen.

Static tensile tests were performed on $25 \text{ mm} \times 200 \text{ mm}$ specimens with a Z250 tensile testing machine (Zwick GmbH & Co., Ulm, Germany) with a crosshead speed of 5 mm/s. The machine equipped with a 250 kN load cell, and the strain was registered with a Mercury Monet DIC (Digital Image Correlation) device (Sobriety, Kurim, Czech

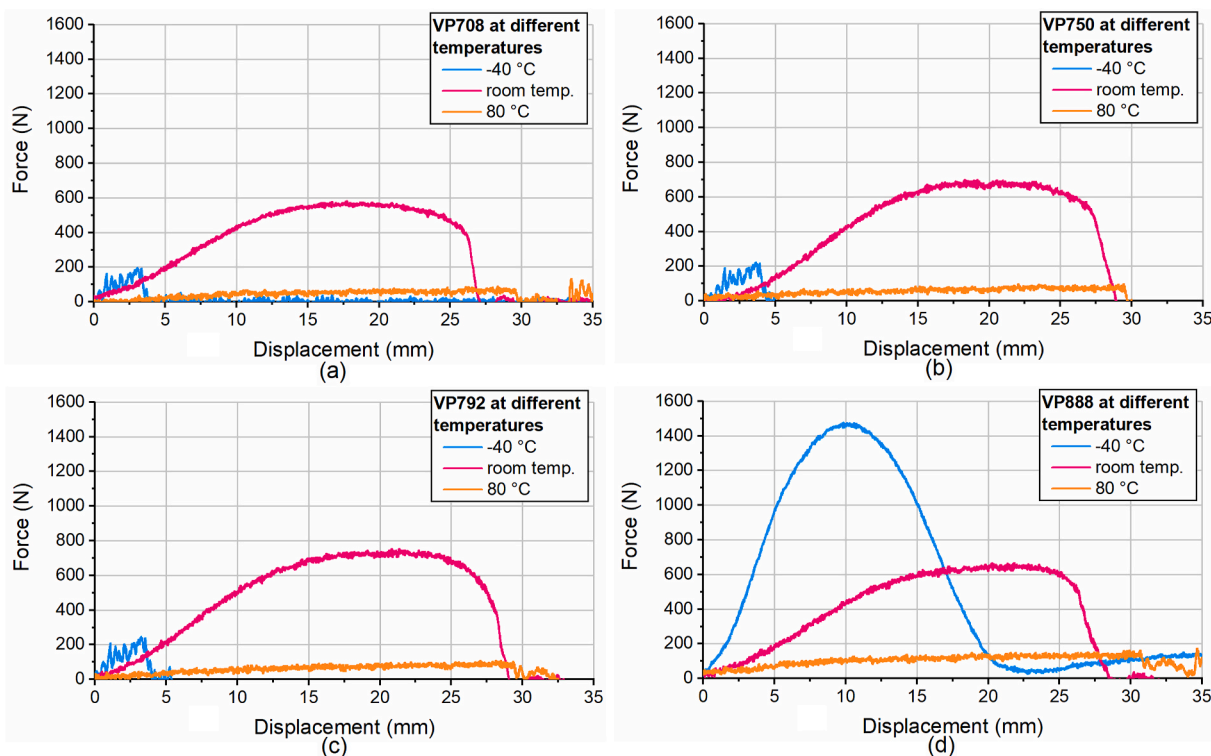


Fig. 4. Typical IFWI curves of VP 708 (a), VP750 (b), VP792 (c), and VP888 (d) matrices at different test temperatures.



Fig. 5. Light microscopic images of VP792 composite consolidated at 120 °C (a), 140 °C (b), and 160 °C (c).

Republic). The tests were conducted at room temperature, -40 °C, and 80 °C.

At least five specimens were tested in all cases.

3. Results and discussion

3.1. Characterization of the raw materials

VP708, VP750, and VP792 showed a small melting peak at around 80 °C (Table 2), consequently, these matrices have a low level of crystallinity. This can be caused by copolymerized isotactic segments. VP888, however, showed two melting peaks: a smaller peak at 105.4 °C and another at 160.8 °C (Fig. 3). During composite production, as the first melting peak was reached upon heating, VP888 was in a quasi-melted state with very high viscosity. It only became fully melted when it was heated above its second melting peak. This higher melting peak of VP888 corresponds with copolymerized or grafted isotactic PP segments. The other matrices showed significantly lower melting temperatures (Table 2). VP792 showed a cold crystallization peak around room temperature. The melting peak of the reinforcing tape and filament is much higher than the melting peaks of the APAO matrices, so the wide processing window exists. It is important to note that Fig. 3 shows the curves obtained from the 1st and 2nd heating run in the case of the fabrics and the matrices, respectively. The reason for this is that during fabric coating, due to the high pulling speed, the fibers only suffer a mild heat load, but the matrices are in a molten state. Consequently, in composite production, the 1st DSC heating run cannot be applied to the matrices, as they have already been melted once.

At the test temperatures of -40 °C and 80 °C, the matrices showed significantly lower perforation energy than at room temperature (Table 3). At room temperature, VP792 showed the highest perforation energy, which can be attributed to its high molecular weight. VP888 possessed the highest perforation energy at 80 °C because, at this temperature, the other matrices were almost in a molten state. VP888 also showed very high perforation energy at -40 °C, since this test temperature is close to its glass transition temperature. At -40 °C, the other matrices displayed brittle behavior (Fig. 4). VP708, VP750, and VP792 showed similar curves, only VP888 showed a very large energy damping at -40 °C.

3.2. Consolidation of the composites

With increasing consolidation temperature, the reinforcing fabric suffered larger relaxation (Table 4). Still, there are no significant differences between the relaxation of the composites with different matrices prepared at the same temperature. The areal relaxation of the composites was determined with the ratio of the areas of the impregnated pre-product and the composite sheets.

The overall densities are lower than the density of the matrix or the reinforcing fabric (Table 4), indicating that the composites are not

Table 5

The dimensions of the cross-section of the reinforcing tapes of the composites (VP792) consolidated at different temperatures.

Consolidation temperature (°C)	Width (μm)	Thickness (μm)
As-received tape	2534 ± 196	104 ± 4
120	2454 ± 55	109 ± 4
140	2352 ± 90	112 ± 5
160	2181 ± 106	142 ± 15

properly consolidated. On the other hand, with increasing processing temperature, density also increases in the case of VP708, VP750, and VP792. This tendency was caused by the lower viscosity of the melted matrices at higher temperatures, which increased the ability of the matrices to impregnate the fabric properly. On the other hand, VP888 showed the lowest density at the consolidation temperature of 140 °C, which indicates poorer consolidation.

Peel strength increases with increasing consolidation temperature, similarly to density, indicating that the matrix melt showed lower viscosity at higher consolidation temperatures and, consequently, was able to impregnate the fabric better. VP708 and VP888 showed lower peel strength compared to VP750 and VP792. In the case of VP708, this could be caused by the poor mechanical properties of the matrix. On the other hand, the low interlaminar strength of VP888 can be attributed to its poor consolidation.

Fig. 5 shows the light microscopic images of the composites (VP 792) consolidated at 120 , 140 and 160 °C. The tapes cut crosswise are the warp tapes, while the tapes cut lengthwise are the weft tapes. For the weft tapes, the folded structure (seen as multiple parallel layers) is characteristic due to the overfeeding of the weaving process. Significant transversal shrinkage can be seen for composites consolidated at 160 °C, which was manifested in the waviness of the reinforcing tapes along their width. Slight shrinkage can also be detected for those consolidated at 140 °C. The void content of the composites decreased with increasing consolidation temperature.

The relaxation phenomenon changed not only the shape of the tapes but also their size. The dimensions of the tapes measured on the light microscopic cross-section of the composites (VP792) are listed in Table 5. Parallel to the increasing areal relaxation with increasing consolidation temperature, the width of the tapes decreased, and their thickness increased with increasing consolidation temperature. The type of the matrix did not influence the dimensional changes of the cross-section of the tapes, which is in good agreement with the tendency observed in the areal relaxation values.

3.3. Static tensile test

In the case of composites with VP708 and VP888 matrices consolidated at 140 °C, the second section of the tensile curves showed fluctuating stress values, which was caused by delamination (Fig. 6/a). The

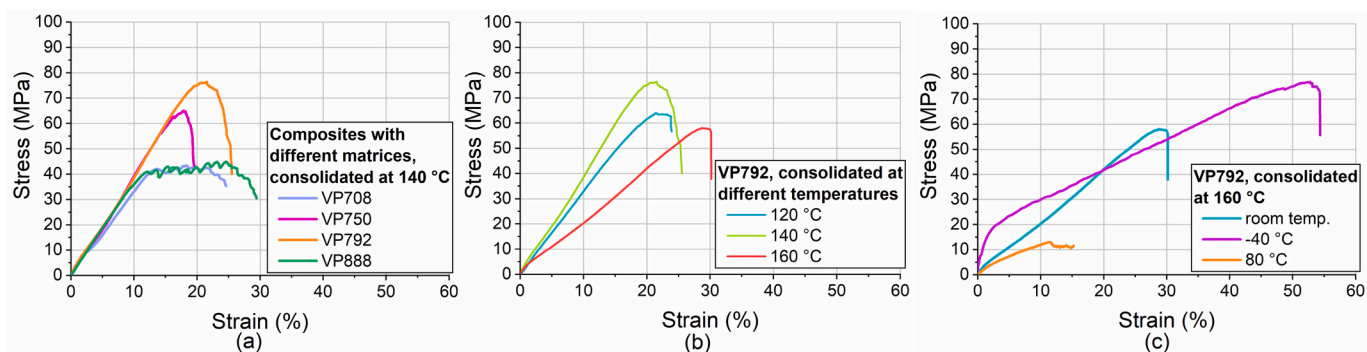


Fig. 6. Typical tensile curves of the composites with different matrices consolidated at 140 °C tested at room temperature (a), the effects of consolidation temperature (b) and the effects of test temperature (c).

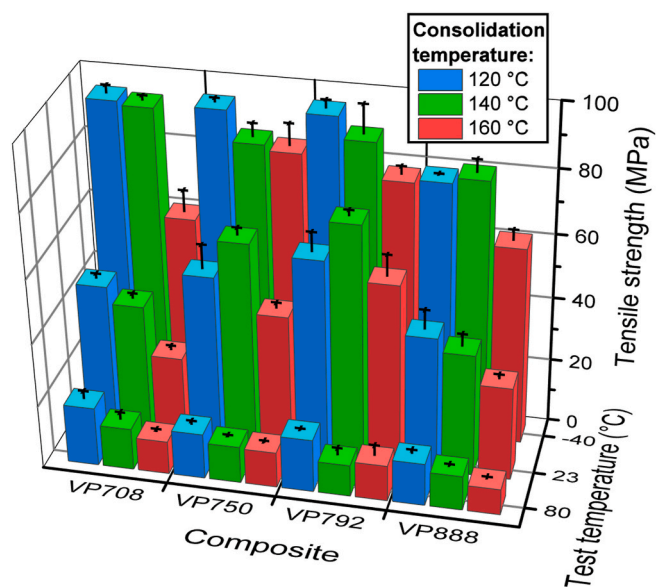


Fig. 7. Tensile strength of the composites.

reason for delamination was the poor adhesion between the matrix and fabric layers in the case of VP708, and the poor consolidation in the case of VP888. The tensile curves of VP750 and VP792 did not show signs of delamination. At the test temperature of 80 °C, the matrices were almost in a molten state. It caused severe delamination, accompanied by a significant loss of strength and the modulus. At the test temperature of -40 °C, a change is observable in the steepness of the curve up to 2% strain. At the start of loading SPCs, the matrix was stiff and worked well

with the reinforcing fabric. At a certain load level, the matrix suffered brittle failure (it has a smaller failure strain than the fiber at -40 °C). After matrix failure, the reinforcing fabric layers were able to move and be deformed more freely, resulting in a larger failure strain of the composite. This phenomenon was characteristic of all PP-SPCs studied.

At room temperature (Fig. 7), the VP750 and VP792 composites consolidated at 140 °C showed the highest tensile strength. The possible reason for this behavior is that with increasing consolidation temperature, the following effects occur: (i) the viscosity of the matrix melt decreases, improving its capability to impregnate the fabric, thus, improving the consolidation of the composite; (ii) the heat load of the reinforcing fabric also increases, accelerating molecular relaxation, thereby reducing its reinforcing ability, thus, deteriorating the tensile properties of the composite. These phenomena affect the properties of the composites in the opposite direction, and in the case of VP750 and VP792, the optimum of these effects occurred around 140 °C. In the case of VP708 and VP888, tensile strength decreased with increasing consolidation temperature. For VP708, the possible reason for this tendency is that VP708 has by far the lowest viscosity compared to the other matrices; thus, it was able to properly impregnate the fabric at 120 °C, so increasing the processing temperature did not result in a further increment in consolidation. Consequently, the properties of the composite were mainly affected by the relaxation of the fabric at elevated temperatures. The tensile strength of the composites with the VP708 matrix was relatively low, due to the poor adhesion between the matrix and the reinforcing fabrics caused by the low molecular weight of VP708. VP888 showed similar behavior, but because the matrix was not able to properly impregnate the reinforcing fabric due to its low viscosity.

At the test temperature of -40 °C, the tensile strength of all the composites decreased with increasing consolidation temperature. Because of the brittle behavior of the matrices below T_g , they were not able to properly transfer the load to the reinforcement; and the composite lost its structural integrity early in the test. Thus, the tensile

Table 6
Tensile modulus of the composites.

Matrix	Consolidation temperature (°C)	Tensile modulus (MPa)		
		at -40 °C	at room temperature	at 80 °C
VP708	120	1334 ± 87	610 ± 39	175 ± 22
VP708	140	1003 ± 178	492 ± 30	147 ± 13
VP708	160	1356 ± 99	339 ± 29	83 ± 1
VP750	120	854 ± 182	529 ± 61	128 ± 8
VP750	140	1103 ± 159	354 ± 46	111 ± 4
VP750	160	1058 ± 183	325 ± 17	80 ± 18
VP792	120	1328 ± 39	443 ± 63	140 ± 19
VP792	140	1223 ± 94	475 ± 40	98 ± 6
VP792	160	1245 ± 259	368 ± 15	103 ± 31
VP888	120	895 ± 48	496 ± 26	133 ± 20
VP888	140	758 ± 48	285 ± 34	98 ± 10
VP888	160	798 ± 68	240 ± 27	62 ± 6

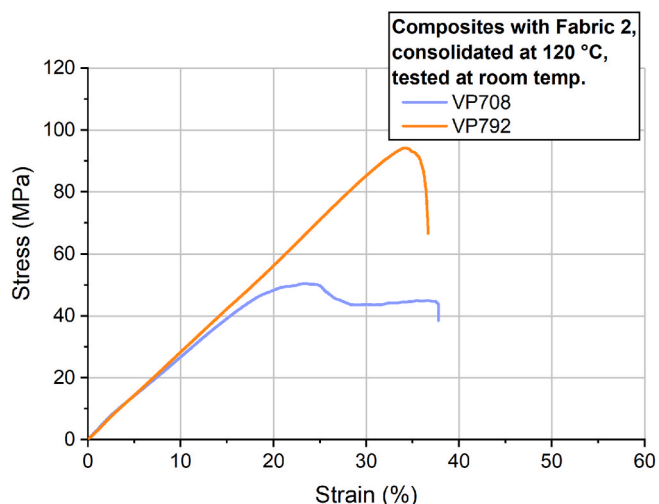


Fig. 8. Typical tensile curves of the composites made with Fabric 2.

Table 7
The tensile properties of the composites with Fabric 2.

Matrix	Tensile strength (MPa)	Tensile modulus (MPa)
VP708	47.4 ± 1.5	56.1 ± 2.1
VP792	62.6 ± 6.0	99.4 ± 4.6

properties are mainly determined by the relaxation of the fabric, and not by the quality of consolidation. Consequently, as the reinforcing fabric suffered more relaxation at higher temperatures, the tensile strength of the composites decreased with increasing processing temperature. Nevertheless, as the test temperature of -40 °C is also below the T_g of the fabric, at this temperature, the overall tensile properties are better compared to those measured at room temperature.

The test temperature of 80 °C was closer to the melting temperature of the matrices, so the properties of the composites were also mainly affected by the more significant relaxation of the fabric at higher consolidation temperatures. At 80 °C, overall tensile strength was lower than at room temperature, because, at this test temperature, the reinforcing fabric was more ductile.

At room temperature, the modulus decreased with increasing consolidation temperature (Table 6), due to more relaxation of the fabric at higher processing temperatures. At -40 °C, the tensile modulus was significantly higher than at room temperature, as the test temperature is below the T_g of both the reinforcement and the matrices. Due to the relatively high deviation in the case of the test temperature of -40 °C, the effect of consolidation temperature could not be examined. At the

testing temperature of 80 °C, the modulus was smaller than at room temperature, since 80 °C is close to the melting temperatures of the matrices. At 80 °C, increasing consolidation temperature decreased the modulus because of the increased relaxation of the reinforcing fabric.

In the case of VP708 made with Fabric 2, a plateau is observable on the tensile curve after it reached its maximum (Fig. 8). It can be attributed to the delamination that occurred in the composite, caused by the poor mechanical properties of the VP708 matrix. In the case of VP792, there is no detectable sign of delamination, and the maximal strength is higher compared to VP708.

The tensile strength of the composites can be enhanced by using a fabric with better properties, especially in the case of the VP792 matrix (Table 7). VP792 combined with Fabric 2 showed the maximal tensile strength of 99.4 MPa. This value is somewhat lower than that of the commercially available SPCs (e.g. 120 MPa for Curv® [37] and 207 MPa for Tegriss® [38]). The tensile modulus of composites with Fabric 2 considerably decreased. This can be attributed to the different properties of Fabric 2.

3.4. Falling weight impact tests

At room temperature, perforation energy decreased with increasing consolidation temperature, and the typical failure behavior is fiber breakage (Figs. 9 and 10). It can be attributed to the energy damping capacity of delamination, which was reduced with increasing processing temperatures due to better consolidation. The composites with the VP888 matrix consolidated at 120 °C and 140 °C showed considerably higher perforation energy than the other matrices, indicating poor consolidation (Fig. 11).

A similar tendency is observable at the test temperature of -40 °C, but the perforation energies are higher, as the matrices were below their T_g, which caused brittle matrix behavior. Because of this, the matrix layers bonding the fabric layers together suffered a brittle fracture upon impact loading. Thus, the reinforcing fabric layers showed larger deformation until their perforation. This, combined with the higher tensile strength of the reinforcement below T_g, resulted in higher perforation energy values of the composites.

The highest perforation energy values were measured at 80 °C (Fig. 11) with the composites consolidated at 120 °C and 140 °C, because, at this test temperature, the VP708, VP750, and VP792 matrices were almost in a molten state, which resulted in more significant delamination, hence, increased perforation energy. In the case of the composites consolidated at 160 °C, perforation energy dropped at the test temperature of 80 °C. Although the reason for this decrement is not clear yet, it may be attributed to the matrix film on the surface of the specimens. At the consolidation temperature of 160 °C, the viscosity of the matrices was low enough, therefore the matrices were not only able to fully impregnate the fabric, but also flowed through the outer fabric

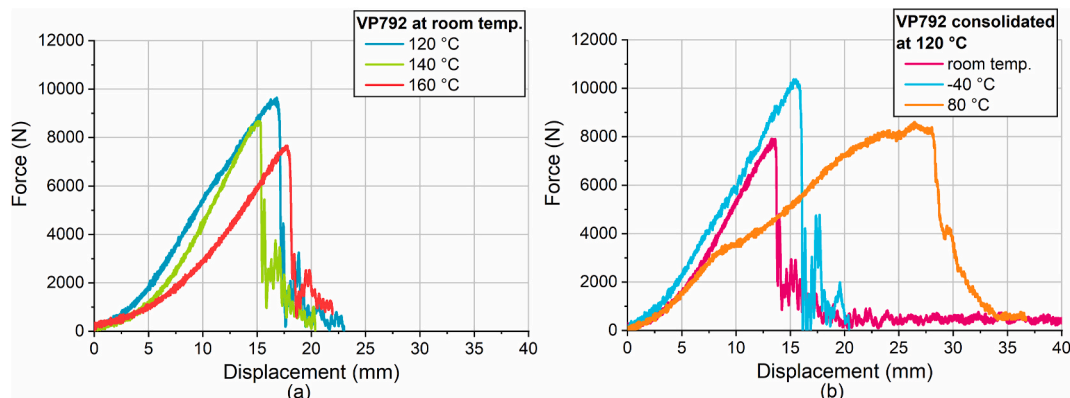


Fig. 9. Typical IFWI curves of the VP792 composites tested at room temperature (a), and the effect of the test temperature (b).

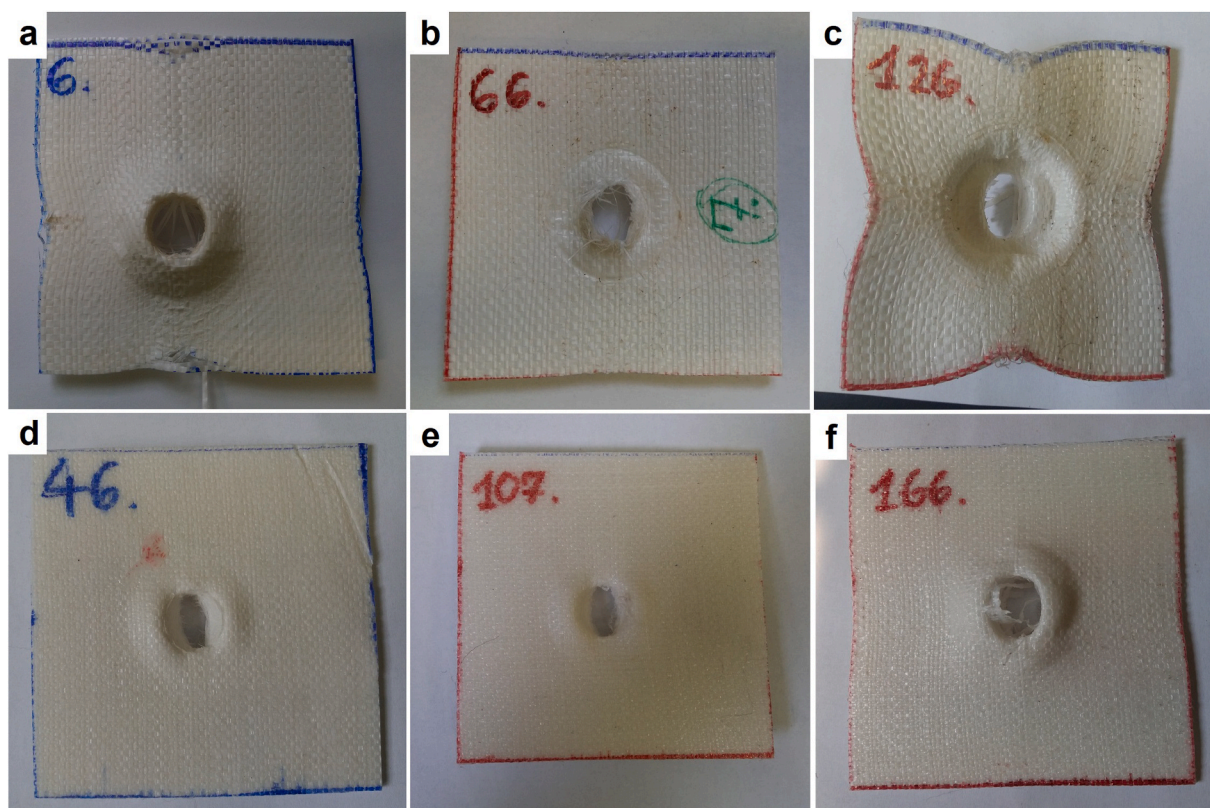


Fig. 10. Typical failure behavior of composites with Fabric 1 and the VP750 matrix consolidated at 120 °C at the test temperatures of -40 °C (a), 23 °C (b), and 80 °C (c) and the composites with the same components consolidated at 160 °C at the test temperatures of -40 °C (d), 23 °C (e) and 80 °C (f).

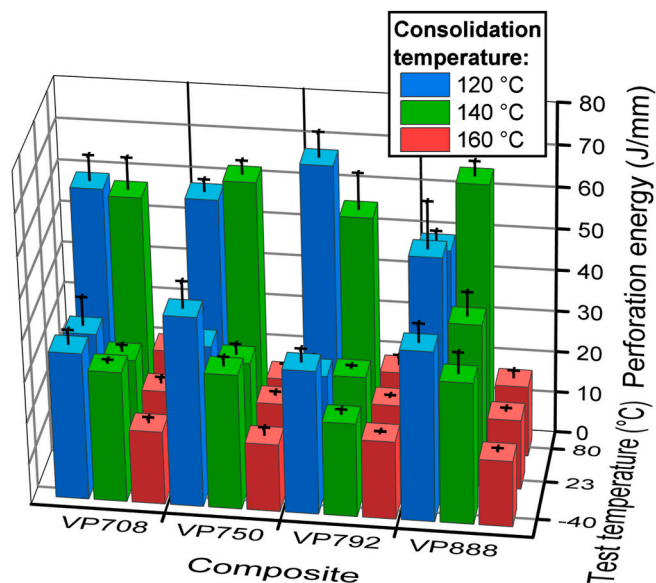


Fig. 11. Perforation energy of the composites.

layer, forming a thin matrix layer on the surface of the composites (Fig. 12). It is possible that this matrix layer acted as an adhesive (the applied matrices were initially invented for melt adhesive purposes), decreasing the relative displacement between the specimens and the grip, thus reducing perforation energy.

At the test temperatures of -40 °C and 80 °C, delamination is also detectable (Fig. 10). At 80 °C, the specimens were deformed by the dart upon impact, which increased the registered perforation energy. The composites consolidated at 160 °C showed less deformation due to their

better consolidation, and they showed fiber breakage instead of fiber pull-out, even at the test temperature of 80 °C. Although only the composites prepared with the VP750 matrix are shown in Fig. 9, the composites produced with the other matrices showed similar failure behavior.

The impact behavior of the composites prepared with Fabric 2 was also strongly influenced by the test temperature (Fig. 13). At the test temperature of -40 °C, the typical failure behavior was fiber breakage (Fig. 14). At room temperature, the specimens were partially deformed upon impact, and delamination is also detectable. At 80 °C, the dart did not fully penetrate the specimens, and the specimens were severely deformed.

In the case of composites produced with Fabric 2, perforation energy is higher, thus the impact properties of the composites can be improved by using a high-performance fabric. At room temperature, although the specimens were perforated, the tapes in the middle were pulled in the ring, as the pressure of our apparatus was not enough to maintain the initial position of the samples, and this caused bigger displacement (Fig. 13). Although this relative movement of the specimens caused an increment in the registered perforation energy, it also proves that the composites had high strength and excellent energy damping ability.

4. Conclusions

We prepared polypropylene-based single-polymer composites using amorphous poly-alpha-olefins (APAOs) as matrices, to investigate the possibility of widening the processing window by exploiting the low melting temperature of APAOs. Two reinforcing fabrics (one composed of highly stretched split PP tapes, the other of high-strength PP multifilaments) were tested with four different APAO-based melt adhesives (VP708, VP750, VP792, and VP888) as matrices. We designed and built a fabric conveying device to directly coat the fabric with the matrices to avoid high deviation in the fiber content of the composites and make

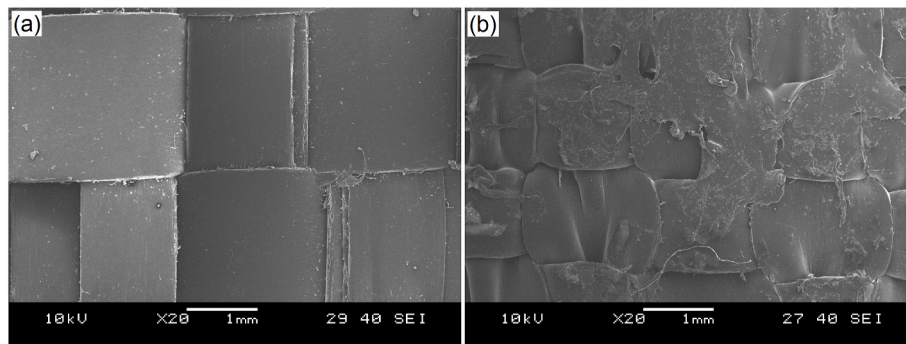


Fig. 12. Scanning electron microscopic pictures of the VP792 composite consolidated at 120 °C (a) and 160 °C (b).

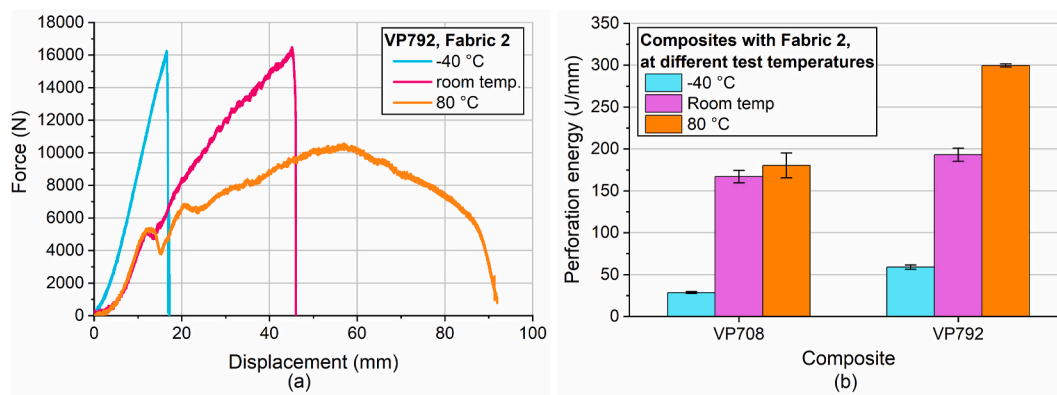


Fig. 13. Typical IFWI curves of the VP792 composite made with Fabric 2 (a) and perforation energy of the composites produced with Fabric 2 (b) at different test temperatures.

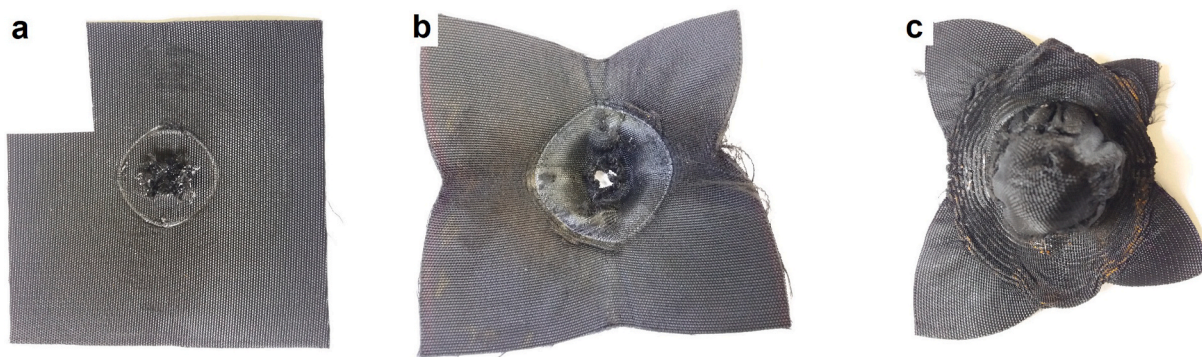


Fig. 14. Typical failure behavior of composites with Fabric 2 and the VP 708 matrix at the test temperatures of $-40\text{ }^{\circ}\text{C}$ (a), $23\text{ }^{\circ}\text{C}$ (b), and $80\text{ }^{\circ}\text{C}$ (c).

production easier. The composites were produced according by film-stacking at the consolidation temperatures of $120\text{ }^{\circ}\text{C}$, $140\text{ }^{\circ}\text{C}$, and $160\text{ }^{\circ}\text{C}$. We performed static tensile and instrumented falling weight impact (IFWI) tests on the composites at room temperature, $-40\text{ }^{\circ}\text{C}$ and $80\text{ }^{\circ}\text{C}$.

We found that the direct coating of the reinforcing fabric is a productive way to produce single-polymer composites with an APAO matrix, and the deviation of the fiber content can also be reduced with it. The processing temperature window can be widened by using the investigated low-melting-point APAO-grades as matrices, and with increasing processing temperature, the consolidation of the composites increased. We found that the optimal processing temperature is roughly between $120\text{ }^{\circ}\text{C}$ and $140\text{ }^{\circ}\text{C}$ for VP750 and VP 792, at around $160\text{ }^{\circ}\text{C}$ for VP888, while the optimal processing temperature for VP708 is below

$120\text{ }^{\circ}\text{C}$. Considering that the melting temperature of the reinforcing fabrics was around $170\text{ }^{\circ}\text{C}$, the processing temperature window can reach $30\text{--}40\text{ }^{\circ}\text{C}$ in the case of VP750 and VP792, and even $50\text{ }^{\circ}\text{C}$ for VP708.

Of the studied matrix materials, the APAO with the highest molecular weight (VP792) seems to be the most promising, which, combined with Fabric 2, showed the maximal tensile strength of $99,4\text{ MPa}$. It is possible, however, that the maximal strength of these composites can be enhanced by applying higher pressure, and thus, further curbing the relaxation of the fabric ($0,6\text{ MPa}$ was the maximal adjustable pressure of the DBP). On the other hand, the perforation energy of these APAO-based SPCs is superior compared to that of the SPCs that are commercially available, even for well-consolidated composites [9].

Declaration of competing interest

The authors declare that they have no known competing financial interests or personal relationships that could have appeared to influence the work reported in this paper

Acknowledgments

The authors are thankful to Evonik Resource Efficiency GmbH for the support and for Meshlin Composites Zrt. for the possibility of using the Double Belt Press for composite production. This work was also supported by BME Nanotechnology and Materials Science TKP2020 IE grant of NKFIH Hungary (BME IE-NAT TKP2020). L. J. Varga thanks for the support of the ÚNKP-19-2 New National Excellence Program of the Ministry for Innovation and Technology.

References

- [1] T. Czigány, Disposable or single-use plastics? Neither! Recyclable or reusable plastics!, *Express Polym. Lett.* 14 (1) (2020) 1.
- [2] G. Marosi, Plastics as target for environmental activists – crisis or challenge? *Express Polym. Lett.* 12 (11) (2018) 957.
- [3] K. Shanmugam, V. Gadhamshetty, P. Yadav, D. Athanassiadis, M. Tysklind, V.K. K. Upadhyayula, Advanced high strength steel and carbon fiber reinforced polymer composite body in white for passenger cars: environmental performance and sustainable return on investment under different propulsion modes, *Sustain. Chem. Eng.* 7 (5) (2019) 4951–4963.
- [4] V. Volpe, S. Lanzillo, F. Affinita, B. Villacci, I. Macchiarolo, R. Pantani, Lightweight high-performance polymer composite for automotive applications, *Polymers* 11 (2) (2019) 326–338.
- [5] Polypropylene Handbook. Morphology, Blends and Composites, in: J. Karger-Kocsis, T. Bárány (Eds.), (eds.), Springer Nature, Cham, Switzerland, 2019.
- [6] M. Prox, B. Pornnimit, J. Varga, G.W. Ehrenstein, Thermoanalytical investigations of self-reinforced polyethylene, *J. Therm. Anal.* 36 (1990) 1675–1684.
- [7] J. Karger-Kocsis, T. Bárány, Single-polymer composites (SPCs): status and future trends, *Compos. Sci. Technol.* 92 (2014) 77–94.
- [8] K. Gawdzinska, M. Nabialek, A.V. Sandu, Bk, The choice of recycling methods for single-polymer polyester composites, *Mater. Plast.* 55 (4) (2018) 658–665.
- [9] T. Bárány, A. Izer, T. Czigány, On consolidation of self-reinforced polypropylene composites, *Plastics, Rubber and Composites* 35 (9) (2006) 375–379.
- [10] N.J. Capiati, R.S. Porter, The concept of one polymer composites modelled with high-density polyethylene, *J. Mater. Sci.* 10 (1975) 1671–1677.
- [11] P.J. Hine, I.M. Ward, N.D. Jordan, R. Olley, D.C. Bassett, The hot compaction behavior of woven oriented polypropylene fibers and tapes. I. Mechanical properties, *Polymer* 44 (4) (2003) 1117–1131.
- [12] P.J. Hine, I.M. Ward, R.H. Olley, D.C. Bassett, The hot compaction of high modulus melt-spun polyethylene fibers, *J. Mater. Sci.* 28 (1993) 316–324.
- [13] N.D. Jordan, D.C. Bassett, R.H. Olley, P.J. Hine, I.M. Ward, The hot compaction behavior of woven oriented polypropylene fibers and tapes. II. Morphology of cloths before and after compaction, *Polymer* 44 (4) (2003) 1133–1143.
- [14] I.M. Ward, P.J. Hine, Novel composites by hot compaction of fibers, *Polym. Eng. Sci.* 37 (11) (1997) 1809–1814.
- [15] D. Zherebtsov, D. Chukov, V. Torokhov, E. Statnik, Manufacturing of single-polymer composite materials based on ultra-high molecular weight polyethylene fibers by hot compaction, *J. Mater. Eng. Perform.* 29 (2020) 1522–1527.
- [16] B. Alcock, N.O. Cabrera, N.-M. Barkoula, J. Loos, T. Peijs, Interfacial properties of highly oriented coextruded polypropylene tapes for the creation of recyclable all-polypropylene composites, *J. Appl. Polym. Sci.* 104 (1) (2007) 118–129.
- [17] J.K. Kim, W.-R. Yu, P. Harrison, Optimum consolidation of self-reinforced polypropylene composite and its time-dependent deformation behavior, *Compos. Appl. Sci. Manuf.* 39 (10) (2008) 1597–1605.
- [18] T. Peijs, Composites for recyclability, *Mater. Today* 6 (2003) 30–35.
- [19] T. Bárány, A. Izer, T. Czigány, High performance self-reinforced polypropylene composites, *Mater. Sci. Forum* 537–538 (2007) 121–128.
- [20] J.C. Chen, C.M. Wu, F.C. Pu, C.H. Chiu, Fabrication and mechanical properties of self-reinforced poly(ethylene terephthalate) composites, *Express Polym. Lett.* 5 (3) (2011) 228–237.
- [21] S. Houshyar, R.A. Shanks, Tensile properties and creep response of polypropylene fiber composites with variation of fiber diameter, *Polym. Int.* 53 (11) (2004) 1752–1759.
- [22] J. Andrzejewski, P. Przyszczypkowski, M. Szostak, Development and characterization of poly(ethylene terephthalate) based injection molded self-reinforced composites, Direct reinforcement by overmolding the composite inserts, *Materials and Design* 153 (2018) 273–286.
- [23] J. Andrzejewski, M. Szostak, J. Krasucki, M. Barczewski, T. Sterzynsky, Development and characterization of the injection-molded polymer composites made from bicomponent fibers, *Polym. Technol. Eng.* 55 (1) (2015) 33–46.
- [24] J. Andrzejewski, N. Tutak, M. Szostak, Polypropylene composites obtained from self-reinforced hybrid fiber system, *J. Appl. Polym. Sci.* 133 (15) (2015).
- [25] I.M. Ward, P.J. Hine, The science and technology of hot compaction, *Polymer* 45 (5) (2004) 1413–1427.
- [26] S. Houshyar, R.A. Shanks, Morphology, thermal and mechanical properties of poly(propylene) fiber-matrix composites, *Macromol. Mater. Eng.* 288 (2003) 599–606.
- [27] C.M. Wu, P.C. Lin, C.T. Tsai, Fabrication and mechanical properties of self-reinforced polyester composites by double covered uncommingled yarn, *Polym. Compos.* 37 (12) (2016) 3331–3340.
- [28] J.M. Zhang, C.T. Reynolds, T. Peijs, All-poly(ethylene terephthalate) composites by film stacking of oriented tapes, *Compos. Appl. Sci. Manuf.* 40 (11) (2009) 1747–1755.
- [29] A. Izer, T. Bárány, J. Varga, Development of woven fabric reinforced all-polypropylene composites with beta nucleated homo- and copolymer matrices, *Compos. Sci. Technol.* 69 (13) (2009) 2185–2192.
- [30] T.N. Abraham, S.D. Wanjale, T. Bárány, J. Karger-Kocsis, Tensile mechanical and perforation impact behavior of all-PP composites containing random PP copolymer as matrix and stretched PP homopolymer as reinforcement: effect of β nucleation of the matrix, *Compos. Appl. Sci. Manuf.* 40 (5) (2009) 662–668.
- [31] A. Izer, A. Stocchi, T. Bárány, V. Pettarin, C. Bernal, T. Czigány, Effect of the consolidation degree on the fracture and failure behavior of self-reinforced polypropylene composites as assessed by acoustic emission, *Polym. Eng. Sci.* 50 (11) (2010) 2106–2113.
- [32] A. Stocchi, V. Pettarin, A. Izer, T. Bárány, T. Czigány, C. Bernal, Fracture behavior of recyclable all-polypropylene composites composed of α - and β -modifications, *J. Thermoplast. Compos. Mater.* 24 (6) (2011) 805–817.
- [33] T. Bárány, A. Izer, A. Menyhárd, Reprocessability and melting behavior of self-reinforced composites based on PP homo and copolymers, *J. Therm. Anal. Calorim.* 101 (1) (2010) 255–263.
- [34] J. Varga, β -modification of isotactic polypropylene: preparation, structure, processing, properties and application, *J. Macromol. Sci., Part B: Physics* 41 (4–6) (2002) 1121–1171.
- [35] A. Sustic, Amorphous Poly Alpha Olefin (APAO) Based Hot Melts, ASC Hot Melt Short Course, New Orleans, United States, 2016.
- [36] L.J. Varga, T. Bárány, Development of polypropylene-based single-polymer composites with blends of amorphous poly-alpha-olefin and random polypropylene copolymer, *Polymers* 12 (6) (2020) 1429.
- [37] G. Romhány, T. Bárány, T. Czigány, J. Karger-Kocsis, Fracture and failure behavior of fabric-reinforced all-poly(propylene) composite (Curv), *Polym. Adv. Technol.* 18 (2007) 90–96.
- [38] S. Valluri, S. Sankaran, P.K. Mallick, Tensile and Fatigue Performance of a Self-Reinforced Polypropylene, Automotive Composites Conference and Exhibition, Society of Plastics Engineers, Dearborn, United States, 2010.